H-Bonded Effects on Novel Supramolecular Dendrimers Containing Electron-Transporting Donor Dendrons and Single/Double H-Bonded Acceptor Emitters

Chung-Wen Wu and Hong-Cheu Lin*

Department of Materials Science and Engineering, National Chiao Tung University, Hsinchu, Taiwan (ROC)

Received May 9, 2006; Revised Manuscript Received September 1, 2006

ABSTRACT: Novel asymmetric/symmetric supramolecular dendrimers were constructed by two kinds of (single/double) H-bonded acceptor chromophores, i.e., pyridyl/bispyridyl acceptor emitters, encapsulated with (one or two) 1,3,4-oxadiazole (OXD) donor dendrons in proper acceptor/donor molar ratios. These acceptor emitters were also complexed with another type of dendritic donor cores to form exterior emitting shells reverse to the previous system (with emitting cores) via self-assembly of complementary H-bonded moieties. Because of the shielding effect of bulky OXD dendritic shells in H-bonded donors, the supramolecular dendrimers are able to prevent acceptor emitters from spatial aggregation, and thus to induce glass-forming properties (with T_g) and show stronger emission intensities via H-bonds. Besides, the dendritic donors act as efficient light-harvesting antennae capable of transferring light energy from their peripheral OXD arms to their emitting acceptors, where the chromophore luminance induced by energy transfer is more efficient than that by direct excitation of the emitting cores. Compared with analogous dendritic mixtures without H-bonds, higher quantum yields were observed in the supramolecular dendrimers because of better energy transfer from OXD units. Therefore, compared with acceptor emitters, not only can the emission wavelength be tuned (up to 100 nm of red-shift) by H-bonds, but also much higher emission efficiencies of the H-bonded complexes were induced by reduced aggregation and energy transfer from the OXD donor dendrons.

Introduction

In the past decade, electroluminescent materials have attracted significant attention since the first contribution of small molecular organic light-emitting diodes (OLED) by Tang[1] et al. and polymeric light-emitting diodes (PLED) by Friend[2] et al. Because of their enormous potential applications in flat panel displays, great efforts have been paid to develop novel electroluminescent materials with intense luminescent efficiencies, good thermal/electrical/optical stabilities, and desirable film morphology.[3−7]

The luminescent quantum efficiencies of π-conjugated materials are substantially lower in the solid state than those in the solution state because of intermolecular interactions, such as aggregation and excimer formation, which lead to a self-quenching process of excitons.[8,9] A very attractive way to solve this problem is to encase chromophores within dendritic architectures.[10,11]By connecting bulky dendrons around a central dye moiety, it has been used to prevent the self-aggregation of chromophores in the solid state[12,13] and also define the color of the light emission.[14] Furthermore, chromophore-cored dendrimers may be potentially useful as multifunctional emissive materials in OLED devices. For example, the proper charge transporting functionalities are incorporated at the periphery of the dendritic wedges. This may result in the improvement of imbalanced charge characters in organic luminescent materials.[15,16] In light-harvesting antennae, the peripheral donor units can collect photons, and transfer excitation energy through bonds to the cores or focal points of the acceptors, thus to enhance luminescence efficiencies considerably. In addition, a special benefit is that the amorphous phase of chromophores can be significantly induced by well-defined dendritic structures which prevent from crystallization of chromophores to develop high quality films by spin-coating technique. It is important because melting and recrystallization, caused by heat or short-circuit currents, often result in device damages.[17−19]

Another route to overcome the π-π stacking phenomenon is the utilization of branching systems. In a previous report, oligo(*p*-phenylenevinylene)s (OPVs) have been oriented in a tetrahedral framework to minimize the intramolecular stacking.[20] These tetrahedral arrays do not crystallize and thus form stable amorphous phases. However, it is very difficult to obtain branched systems because of their complicated synthetic routes and low yields. Supramolecules as well as supramolecular polymers can be prepared from two complementary components that are appropriately substituted with functional H-bonded donor and acceptor groups.[21−23] The simpler synthetic molecules through supramolecular self-assembly often possess specific and useful chemical, physical, or optical properties due to the collective behavior of each other. Upon hydrogen-bonded (H-bonded) complexation with dendritic acceptors, the supramolecular dendrimers showed a significantly higher PL emission than those individual emitting OPV donors alone, due to the three-dimensional orientation of the OPV emitting molecules.[24]

In our previous work,[25] we have completed several series of H-bonded liquid crystalline trimers and H-bonded polymer networks, which were constructed by complexation of two complementary components containing various bifunctional photoluminescent (PL) acceptor cores and monofunctional proton donors (or donor polymers). These supramolecular trimers and H-bonded polymer networks demonstrate that different wavelengths of PL emissions and liquid crystalline phases can be achieved by introducing nonphotoluminescent proton donors (or donor polymers).

* Author for correspondence. Telephone: 8863-5712121 ext. 55305. Fax: 8863-5724727. E-mail: linhc@cc.nctu.edu.tw.

10.1021/ma0610358 CCC: $33.50
Published on Web 10/17/2006

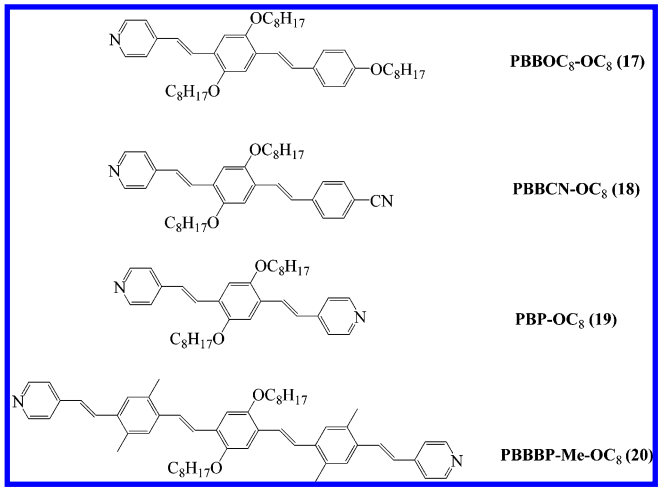

Figure 1. Mono-pyridyl (single H-bonded) and bis-pyridyl (double H-bonded) acceptors used in supramolecular dendrimers.

In this report, the design, synthesis, and optical properties of highly efficient light emitting H-bonded dendrimers with single/double H-bonds, i.e., asymmetric/symmetric supramolecules as shown in Figure 2, are presented. A new strategy involving two complementary segments which contain monofunctional/bifunctional photoluminescent acceptor cores and dendritic donor wedges (bearing OXD segments) are explored. The key structural elements in the dendritic H-donors are various generations of functional poly(aryl ether) dendrons bearing outward OXD arms and a focal point of benzoic acid. This self-assembly of dendritic framework is expected to be effective for the construction of light-harvest of OXD arms and site-isolation of emitting cores. The absorption and emission spectra, as well as energy transfer of the H-bonded dendrimers are also studied to gain insight into the effect of dendritic wedges on the photoluminescent cores. Significantly, by choosing different generations of H-donors, the color of PL emission can be tuned. Even more, stronger fluorescence emission from OXD excitation can be obtained by reduced aggregation and energy transfer from OXD wedges in these supramolecular dendrimers. On the other hand, dendritic donor cores of poly(alkyl aryl ether) were also synthesized to form another chromophore-shelled dendrimers by complexation with the same emitting acceptors (as the peripheral emitting shells) in comparison with the previous chromophore-cored dendrimers. Hopefully, this study is expected to be helpful and constructive for the forthcoming researches about light-emitting dendrimers.

Experimental Section

Measurements and Characterization. ^{1}H NMR spectra were recorded on a Varian Unity 300 MHz spectrometer using $CDCl_3$ or DMSO-d_6 solvent with tetramethylsilane as reference. Elemental analyses were performed on a HERAEUS CHN-OS RAPID elemental analyzer. MALDI−TOF spectra were measured on a Biflex III (Bruker) time-of-flight mass spectrometer utilizing a 5-methoxysalicylic acid matrix. Fourier transform infrared (FTIR) spectra were performed a Nicolet 360 FT-IR spectrometer. Phase transition temperatures were determined by differential scanning calorimetry (Perkin-Elmer Diamond) with a heating and cooling rate of 10 °C/min and polarizing optical microscopy (Leica DMLP) equipped with a hot stage. UV−visible absorption spectra were recorded in dilute THF solutions (10^{-6} M) on a HP G1103A spectrophotometer, and photoluminescence (PL) spectra were obtained on a Hitachi F-4500 spectrophotometer. Thin films of UV−vis and PL measurements were spin-coated on a quartz substrate from THF solution with a concentration of 1 wt %. The fluorescence quantum yields (Φ_{PL}) of the chromophores and H-bonded dendrimers were determined relative to a standard film of 9,10-diphenylanthracene dispersed in PMMA ($\Phi = 0.83$).[26]

Materials. Chemicals and solvents were reagent grades and purchased from Aldrich, ACROS, TCI, and Lancaster Chemical Co. Dichloromathane and THF were distilled to keep anhydrous before use. The other chemicals were used without further purification. All H-bonded dendrimers were prepared by slow evaporation of THF solution containing the mixtures of the acceptor and donor moieties, followed by drying in vacuo. All H-bonded complexes are made up of appropriate (fully H-bonded) molar ratios of acceptor and donor moieties in THF.

Synthesis. Compounds **1**−**3** and **10** were obtained by following the previous literature procedure.[27−28] The synthetic procedures of all donor dendrimers of various generations containing OXD moieties are described in Schemes 1 and 2. Besides, Scheme 3 shows dendritic donor cores, which are H-bonded with emitting acceptor shells. Synthesis and characterization of all mono-pyridyl and bis-pyridyl acceptor chromophores **PBBOC$_8$-OC$_8$** (**17**), **PBBCN-OC$_8$** (**18**), **PBP-OC$_8$** (**19**), **PBBBP-Me-OC$_8$** (**20**), and their intermediates (as shown in Figure 1) are described in the Supporting Information.

General Synthetic Procedures of Dendritic Benzoic Acid Methyl Esters (G1COOCH$_3$ (4), G2COOCH$_3$ (5), and G3COOCH$_3$ (6)). A mixture of **1**, **2**, or **3** (2.1 equiv), 3,5-dihydroxybenzoate (1 equiv), K_2CO_3 (2.5 equiv), and 18-crown-6 (0.2 equiv) in dry THF was heated to reflux and stirred under nitrogen for 24 h. The mixture was evaporated to dry under reduced pressure, and the residue was partitioned between water and CH_2Cl_2. Later on, the aqueous layer was extracted with CH_2Cl_2, and the organic layer was dried over $MgSO_4$. Consequently, the crude products **G1COOCH$_3$** (**4**), **G2COOCH$_3$** (**5**), and **G3COOCH$_3$** (**6**) were purified as outlined in the following text.

G1COOCH$_3$ (4). G1COOCH$_3$ (**4**) was purified by column chromatography with EA/CH_2Cl_2 (1:10) to get a white solid. Yield: 63%. ^{1}H NMR (ppm, $CDCl_3$): δ 0.86−0.95 (m, 12H), 1.23−1.54 (m, 16H), 1.70−1.76 (m, 2H), 3.90−3.91 (overlap, 7H), 5.15 (s, 4H), 6.81 (s, 1H), 7.00 (d, J = 9 Hz, 4H), 7.30 (s, 2H), 7.57 (d, J = 8.4 Hz, 4H), 8.04 (d, J = 9 Hz, 4H), 8.13 (d, J = 8.4 Hz, 4H). MS (MALDI−TOF): m/z [MH$^+$] 893.75; calcd m/z [MH$^+$] 893.44. Anal. Calcd for $C_{54}H_{60}N_4O_8$: C, 72.62; H, 6.77; N, 6.27. Found: C, 72.61; H, 6.88; N, 6.44.

G2COOCH$_3$ (5). G2COOCH$_3$ (**5**) was purified by column chromatography with EA/CH_2Cl_2 (1:8) to get a white solid. Yield: 73%. ^{1}H NMR (ppm, $CDCl_3$): δ 0.92−0.97 (m, 24H), 1.33−1.53 (m, 32H), 1.74−1.81 (m, 4H), 3.88−3.92 (overlap, 11H), 5.02 (s, 4H), 5.10 (s, 8H), 6.57 (s, 2H), 6.69 (s, 4H), 6.74 (s,1H), 7.00 (d, J = 8.4 Hz, 8H), 7.26 (s, 2H), 7.55 (d, J = 8.1 Hz, 8H), 8.04 (d, J = 8.1 Hz, 8H), 8.10 (d, J = 7.5 Hz, 8H). MS (MALDI−TOF): m/z [MH$^+$] 1861.23; calcd m/z [MH$^+$] 1861.92. Anal. Calcd for $C_{114}H_{124}N_8O_{16}$: C, 73.53; H, 6.71; N, 6.02. Found: C, 73.75; H, 6.74; N, 6.07.

G3COOCH$_3$ (6). G3COOCH$_3$ (**6**) was purified by column chromatography with THF/CH_2Cl_2 (1:8) to get a white solid. Yield: 70%. ^{1}H NMR (ppm, $CDCl_3$): δ 0.91−0.96 (m, 48H), 1.32−1.54 (m, 64H), 1.70−1.76 (m, 8H), 3.85 (s, 3H), 3.89 (d, J = 5.7 Hz, 16H), 4.96−5.04 (overlap, 28H), 6.50 (s, 2H), 6.52 (s, 4H), 6.62 (s, 4H), 6.65 (s, 8H), 6.71 (s, 1H), 6.98 (d, J = 9 Hz, 16H), 7.23 (s, 2H), 7.50 (d, J = 8.1 Hz, 16H), 8.00 (d, J = 9 Hz, 16H), 8.06 (d, J = 8.4 Hz, 16H). MS (MALDI−TOF): m/z [MH$^+$] 3800.23; calcd m/z [MH$^+$] 3800.59. Anal. Calcd for $C_{234}H_{252}N_{16}O_{32}$: C, 73.95; H, 6.68; N, 5.90. Found: C, 73.78; H, 6.71; N, 5.83.

G1COOH (7). To a solution of **G1COOCH$_3$** (**4**) (1.0 equiv) in THF was added KOH (5 equiv) dissolved in water. A small amount of methanol was then added to the two-phase mixture to afford a homogeneous solution. The reaction was heated at reflux for 24 h. After the solution was cooled to room temperature, hydrochloric acid was added to precipitate the product **G1COOH** (**7**), which was isolated by filtration, washed with water and dried overnight in a vacuum oven. Yield: 80%. ^{1}H NMR (ppm, DMSO-d_6): δ 0.85−0.90 (m, 12H), 1.28−1.45 (m, 16H), 1.68−1.74 (m, 2H), 3.92

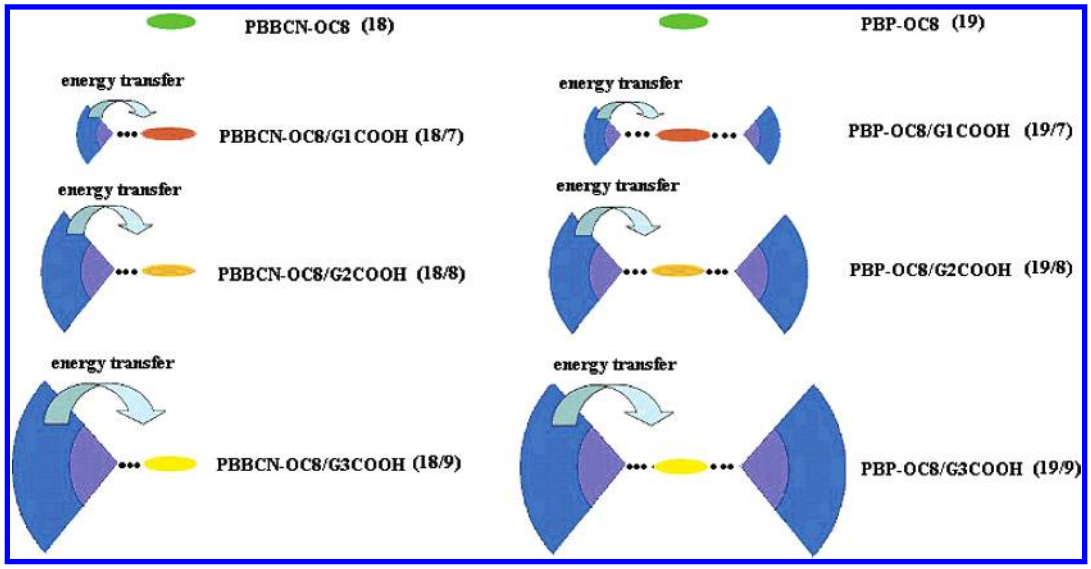

Figure 2. Schematic representation of asymmetric encapsulation of single H-bonded acceptor emitter **PBBCN-OC$_8$** (**18**) and symmetric encapsulation of double H-bonded acceptor emitter **PBP-OC$_8$** (**19**) with different generations (G1-G3) of dendritic donors.

(d, J = 4.8 Hz, 4H), 5.26 (s, 4H), 6.97 (s, 1H), 7.12 (d, J = 8.4 Hz, 4H), 7.19 (s, 2H), 7.65 (d, J = 8.1 Hz, 4H), 8.00 (d, J = 8.7 Hz, 4H), 8.09 (d, J = 7.8 Hz, 4H), 13.10 (broad, COOH). MS (MALDI−TOF): m/z [MH$^+$] 880.53; calcd m/z [MH$^+$] 880.05. Anal. Calcd for $C_{53}H_{58}N_4O_8$: C, 72.42; H, 6.65; N, 6.37. Found: C, 72.04; H, 6.74; N, 6.42.

G2COOH (8). This compound was prepared from **G2COOCH$_3$** (**5**) by the same synthesized procedure as that of **G1COOH** (**8**). Yield: 85%. ^{1}H NMR (ppm, $CDCl_3$): δ 0.90−0.95 (m, 24H), 1.32−1.53 (m, 32H), 1.71−1.75 (m, 4H), 3.86 (d, J = 5.4 Hz, 8H), 5.00 (overlap, 12H), 6.50 (s, 2H), 6.65 (s, 4H), 6.75 (s,1H), 6.96 (d, J = 8.7 Hz, 8H), 7.31 (s, 2H), 7.49 (d, J = 8.1 Hz, 8H), 7.99 (d, J = 8.7 Hz, 8H), 8.05 (d, J = 8.1 Hz, 8H). MS (MALDI−TOF): m/z [MH$^+$] 1848.88; calcd m/z [MH$^+$] 1849.22. Anal. Calcd for $C_{113}H_{122}N_8O_{16}$: C, 73.43; H, 6.65; N, 6.06. Found: C, 73.09; H, 6.93; N, 6.11.

G3COOH (9). This compound was prepared from **G3COOCH$_3$** (**6**) by the same synthesized procedure of **G1COOH** (**9**). Yield: 82%. ^{1}H NMR (ppm, $CDCl_3$): δ 0.90−0.95 (m, 48H), 1.26−1.55 (m, 64H), 1.71−1.75 (m, 8H), 3.86 (d, J = 5.4 Hz, 16H), 4.91−4.98 (overlap, 28H), 6.50 (overlap, 6H), 6.56−6.70 (overlap, 13H), 6.95 (d, J = 8.7 Hz, 16H), 7.27 (s, 2H), 7.47 (d, J = 8.4 Hz, 16H), 7.97 (d, J = 9 Hz, 16H), 8.02 (d, J = 8.4 Hz, 16H). MS (MALDI−TOF): m/z [MH$^+$] 3787.14; calcd m/z [MH$^+$] 3787.57. Anal. Calcd for $C_{233}H_{250}N_{16}O_{32}$: C, 73.91; H, 6.65; N, 5.92. Found: C, 73.63; H, 6.51; N, 6.04.

11. Sodium hydride (3 equiv) in anhydrous THF was slowly added into a stirred solution of compound **10** (1 equiv) in dry THF under nitrogen. After 10 min of stirring, 1,6-dibromohexane (5 equiv) was added rapidly. After being stirred overnight, the reaction mixture was quenched with water. The mixture was evaporated to dry under reduced pressure, and the residue was partitioned between water and CH_2Cl_2. Then, the aqueous layer was extracted with CH_2Cl_2, and the organic layer was dried over $MgSO_4$. Finally, the crude product was purified by column chromatography with CH_2Cl_2/Hexane (1:2) to get a white oil. Yield: 72%. ^{1}H NMR (ppm, $CDCl_3$): δ 1.26−1.44 (m, 4H), 1.57−1.63 (m, 2H), 1.79−1.89 (m, 2H), 3.36−3.45 (m, overlap, 4H), 4.41 (s, 2H), 5.08 (s, 4H), 6.46 (s, 1H), 6.56 (s, 2H), 7.51 (d, J = 8.1 Hz, 4H), 7.65 (d, J = 8.1 Hz, 4H).

12. The previous procedure was followed using sodium hydride (3 equiv), compound **10** (1 equiv), and 1,6-dibromo-decane (5 equiv). The crude product was purified by column chromatography with CH_2Cl_2/Hexane (1:2) to get a white oil. Yield: 67%. ^{1}H NMR (ppm, $CDCl_3$): δ 1.27 (m,12H), 1.55−1.57 (m, 2H), 1.82−1.87 (m, 2H), 3.35−3.44 (m, overlap, 4H), 4.41 (s, 2H), 5.08 (s, 4H), 6.46 (s, 1H), 6.57 (s, 2H), 7.51 (d, J = 7.8 Hz, 4H), 7.66 (d, J = 8.1 Hz, 4H).

General Synthetic Procedures of Dendritic Trialkylated Donor Cores (13 and 14). A mixture of **11** or **12** (3.1 equiv), 1,1,1-tris(4′-hydroxyphenyl)ethane (1.0 equiv), K_2CO_3 (4.0 equiv), and 18-crown-6 (0.3 equiv) in dry THF was heated to reflux and stirred vigorously under nitrogen for 24 h. The mixture was evaporated to dry under reduced pressure, and the residue was partitioned between water and CH_2Cl_2. Then, the aqueous layer was extracted with CH_2Cl_2, and the organic layer was dried over $MgSO_4$. Consequently, the crude products **13** or **14** were purified as outlined in the following text.

13. Compound **13** was purified by column chromatography with EA/CH_2Cl_2 (1:10) to get a slight yellow oil. Yield: 51%. ^{1}H NMR (ppm, $CDCl_3$): δ 1.26−1.43 (m, 12H), 1.57−1.63 (m, 6H), 1.72−1.78 (m, 6H), 2.03 (s, 3H), 3.43 (t, 6H), 3.90 (t, 6H), 4.41 (s, 6H), 5.07 (s, 12H), 6.45 (s, 3H), 6.57 (s, 6H), 6.73 (d, J = 9 Hz, 6H), 6.94 (d, J = 8.4 Hz, 6H), 7.50 (d, J = 8.1 Hz, 12H), 7.65 (d, J = 8.4 Hz, 12H).

14. Compound **14** was purified by column chromatography with EA/CH_2Cl_2 (1:10) to get a slight yellow oil. Yield: 42%. ^{1}H NMR (ppm, $CDCl_3$): δ 1.23−1.40 (m, 36H), 1.55−1.59 (m, 6H), 1.70−1.75 (m, 6H), 2.07 (s, 3H), 3.42 (t, 6H), 3.88 (t, 6H), 4.41 (s, 6H), 5.08 (s, 12H), 6.45 (s, 3H), 6.57 (s, 6H), 6.74 (d, J = 9 Hz, 6H), 6.95 (d, J = 9 Hz, 6H), 7.50 (d, J = 8.4 Hz, 12H), 7.65 (d, J = 8.4 Hz, 12H).

G1-C$_6$-(COOH)$_6$ (15). This compound was prepared from **13** by the same synthesized procedure of **G1-COOH** (**7**). Yield: 77%. ^{1}H NMR (ppm, DMSO-d_6): δ 1.34 (m, 12H), 1.47−1.49 (m, 6H), 1.65 (m, 6H), 1.96 (s, 3H), 3.33 (t, 6H), 3.86 (t, 6H), 4.35 (s, 6H), 5.14 (s, 12H), 6.57 (overlap, 9H), 6.76 (d, J = 8.7 Hz, 6H), 6.85 (d, J = 8.7 Hz, 6H), 7.51 (d, J = 8.1 Hz, 12H), 7.94 (d, J = 7.8 Hz, 12H), 12.94 (broad, COOH). MS (MALDI−TOF): m/z [M$^+$ + K] 1817.14; calcd m/z [M$^+$ + K] 1816.08. Anal. Calcd for $C_{107}H_{108}O_{24}$: C, 72.28; H, 6.12. Found: C, 71.95; H, 6.31.

G1-C$_{10}$-(COOH)$_6$ (16). This compound was prepared from **14** by the same synthesized procedure of **G1COOH** (**7**). Yield: 80%. ^{1}H NMR (ppm, DMSO-d_6): δ 1.21 (m, 36 H), 1.44 (m, 6H), 1.61 (m, 6H), 1.97 (s, 3H), 3.31 (t, 6H), 3.84 (t, 6H), 4.33 (s, 6H), 5.14 (s, 12H), 6.57 (overlap, 9H), 6.75 (d, J = 8.7 Hz, 6H), 6.86 (d, J = 9 Hz, 6H), 7.51 (d, J = 8.1 Hz, 12H), 7.94 (d, J = 8.1 Hz, 12H), 12.94 (broad, COOH). MS (MALDI−TOF): m/z [M$^+$ + K] 1985.31; calcd m/z [M$^+$ + K] 1984.40. Anal. Calcd for $C_{119}H_{132}O_{24}$: C, 73.44; H, 6.84. Found: C, 73.14; H, 6.76.

Scheme 1

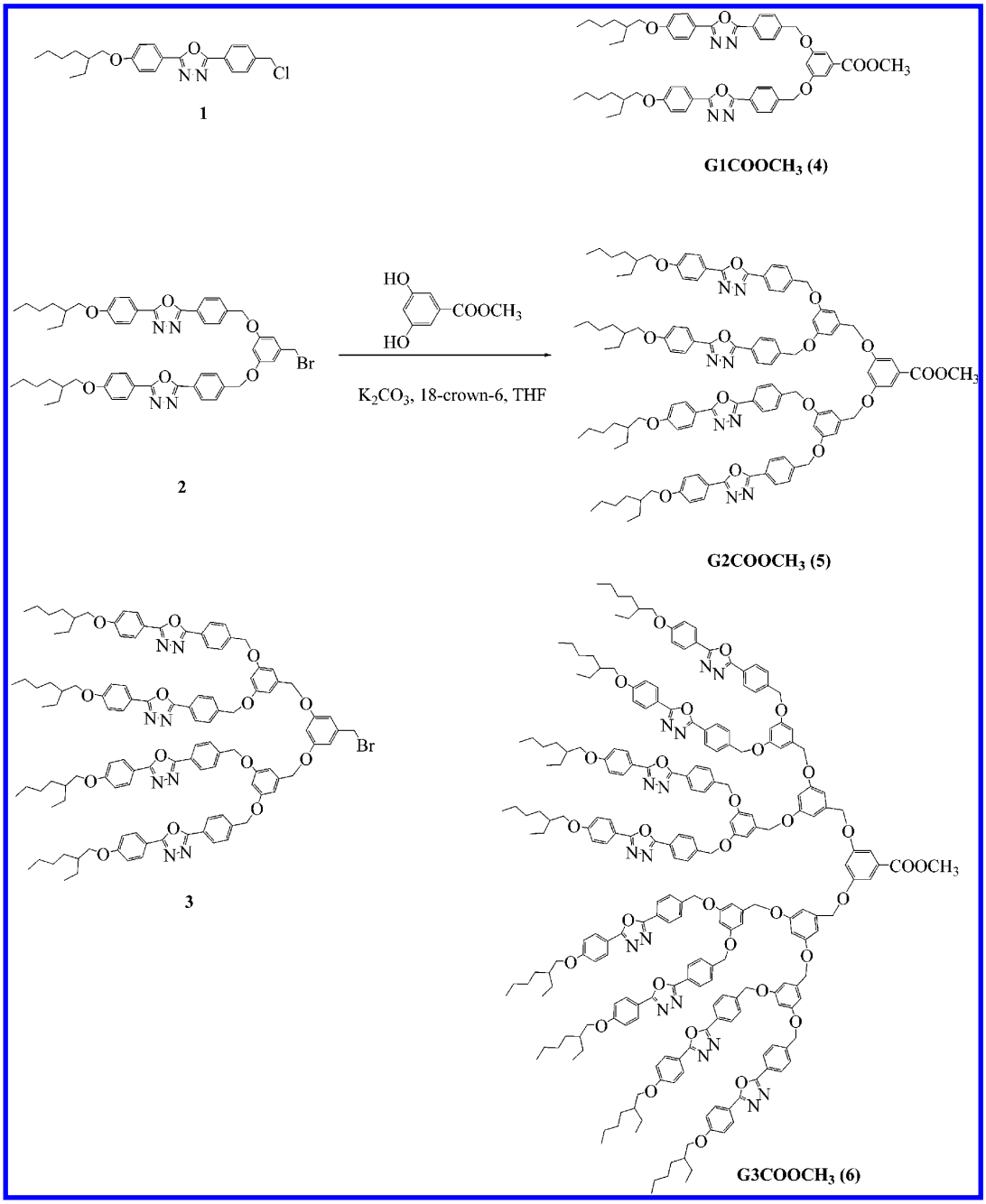

Results and Discussion

Synthesis and Characterization. As shown in Schemes 1−3, all H-bonded donors were synthesized via a previously reported convergent[29] method. In the presence of K_2CO_3 with THF at reflux, 3,5-dihydroxy-benzoic acid methyl ester reacted with various corresponding generations of dendrons (**1**, **2**, and **3**) to obtain **G1COOCH$_3$** (**4**), **G2COOCH$_3$** (**5**), and **G3COOCH$_3$** (**6**), which were followed by hydrolysis reaction with KOH in methanol/THF at reflux to give **G1COOH** (**7**), **G2COOH** (**8**), and **G3COOH** (**9**). Another series of dendrimers (**13** and **14**) were prepared by coupling dendritic wedges to a polyfunctional core and followed by hydrolysis reaction to give **G1-C$_6$-(COOH)$_6$** (**15**) and **G1-C$_{10}$-(COOH)$_6$** (**16**) as shown in Scheme 3. The polyfunctional core chosen in this case was 1,1,1-tris-(4′-hydroxyphenyl)ethane, and the resulting molecules were characterized by NMR spectroscopy, MALDI−TOF mass spectroscopy, and elemental analysis.

All H-bonded complexes are made up of appropriate (fully H-bonded) molar ratios of acceptor and donor moieties in THF. Thus, symmetric supramolecular dendrimers were produced by complexation of double H-bonded acceptor emitters **PBP-OC$_8$** (**19**) and **PBBBP-Me-OC$_8$** (**20**) with dendritic donors **G1COOH** (**7**), **G2COOH** (**8**), and **G3COOH** (**9**) in a molar ratio of 1:2, respectively; and asymmetric supramolecular dendrimers were generated by complexation of single H-bonded acceptor emitters **PBBOC$_8$-OC$_8$** (**17**) and **PBBCN-OC$_8$** (**18**) with dendritic donors **G1COOH** (**7**), **G2COOH** (**8**), and **G3COOH** (**9**) in the molar ratio of 1:1, respectively. Furthermore, the single H-bonded acceptor emitters **PBBOC$_8$-OC$_8$** (**17**) and **PBBCN-OC$_8$** (**18**) were complexed with another type of dendritic donor cores **G1-C$_6$-(COOH)$_6$** (**15**) and **G1-C$_{10}$-(COOH)$_6$** (**16**) in the molar ratio of 6:1 to form exterior emitting shells. In addition, the double H-bonded acceptor emitters **PBP-OC$_8$** (**19**) and **PBBBP-Me-OC$_8$** (**20**) (as H-bonded cross-linkers) were also complexed with

Scheme 2

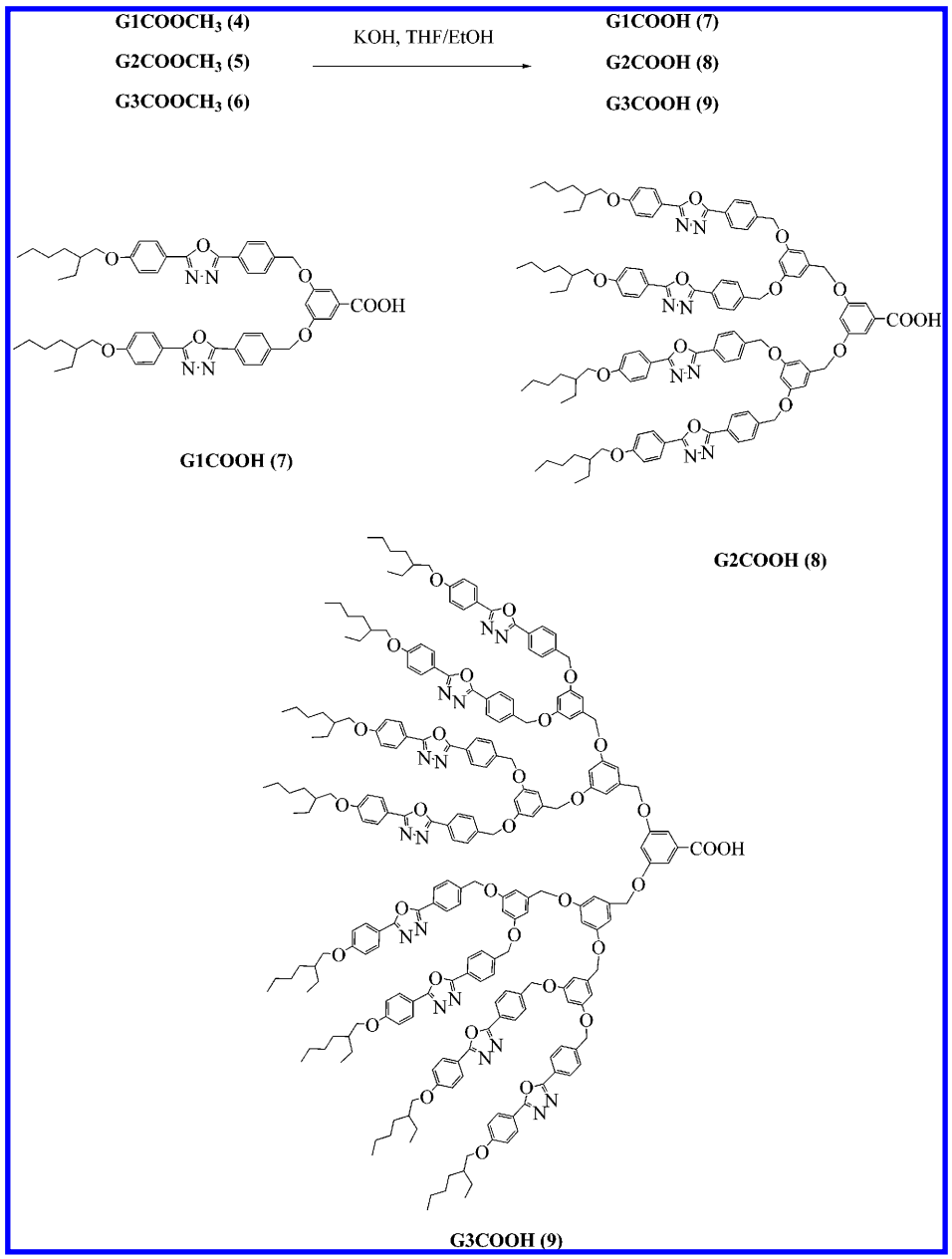

dendritic donor cores **G1-C$_6$-(COOH)$_6$** (**15**) and **G1-C$_{10}$-(COOH)$_6$** (**16**) in the molar ratio of 6:2 to form cross-linked H-bonded emitting shells. The three-dimensional dendritic scaffolding of H-bonded dendrimer design provides the desired amorphous films without crystallization and leads to good film qualities by spin-coating. The resulting supramolecular H-bonded assemblies were investigated with respect to their photophysical and thermal properties.

The existence of hydrogen bonds in the H-bonded complexes can be characterized by IR spectra. Therefore, the IR spectra of **PBBCN-OC$_8$** (**18**), **G1COOH** (**7**), and H-bonded complex of **PBBCN-OC$_8$/G1COOH** (**18/7**) shown in Figure 3 are compared to analyze the hydrogen bonds. In contrast to the O−H band of pure **G1COOH** (**7**) (H-bonded dimer) at 2604 cm^{-1}, the weaker O−H band observed at 1911 and 2500 cm^{-1} in the H-bonded complex **PBBCN-OC$_8$/G1COOH** (**18/7**) is indicative of stronger hydrogen bonding between the pyridyl group of **PBBCN-OC$_8$** (**18**) and the carboxylic acid of **G1COOH** (**7**) in the H-bonded complex. On the other hand, a C═O stretching vibration appeared at 1710 cm^{-1} in the H-bonded complex **PBBCN-OC$_8$/G1COOH** (**18/7**), which show that the carbonyl group was in a less associated state than that in pure **G1COOH** (**7**) (H-bonded dimer) with weaker C═O stretching vibration appeared at 1695 cm^{-1}. Both results suggest that hydrogen bonds formed between **PBBCN-OC$_8$** (**18**) and **G1COOH** (**7**) in the solid state of the H-bonded complex **PBBCN-OC$_8$/G1COOH** (**18/7**). The other H-bonded complexes discussed in this study should have similar consequences as the demonstrated complexes.[30]

Thermal Properties. To elucidate the H-bonding effect on the thermal properties of the H-bonded dendrimers, all compounds were characterized by differential scanning calorimetry (DSC). Polarizing optical microscopy (POM) demonstrated that no phase separation took place between donors and acceptors in the H-bonded dendrimers. In addition, the third-generation (G3) of H-bonded dendrimers containing **G3COOH** (**9**) have higher isotropization temperatures (T_i) than the lower generations of H-bonded dendrimers. As shown in Table 1, it is observed that dendritic donors **G1COOH** (**7**), **G2COOH** (**8**), and **G3COOH** (**9**) possess the glass transition temperatures (Tg) at

Scheme 3

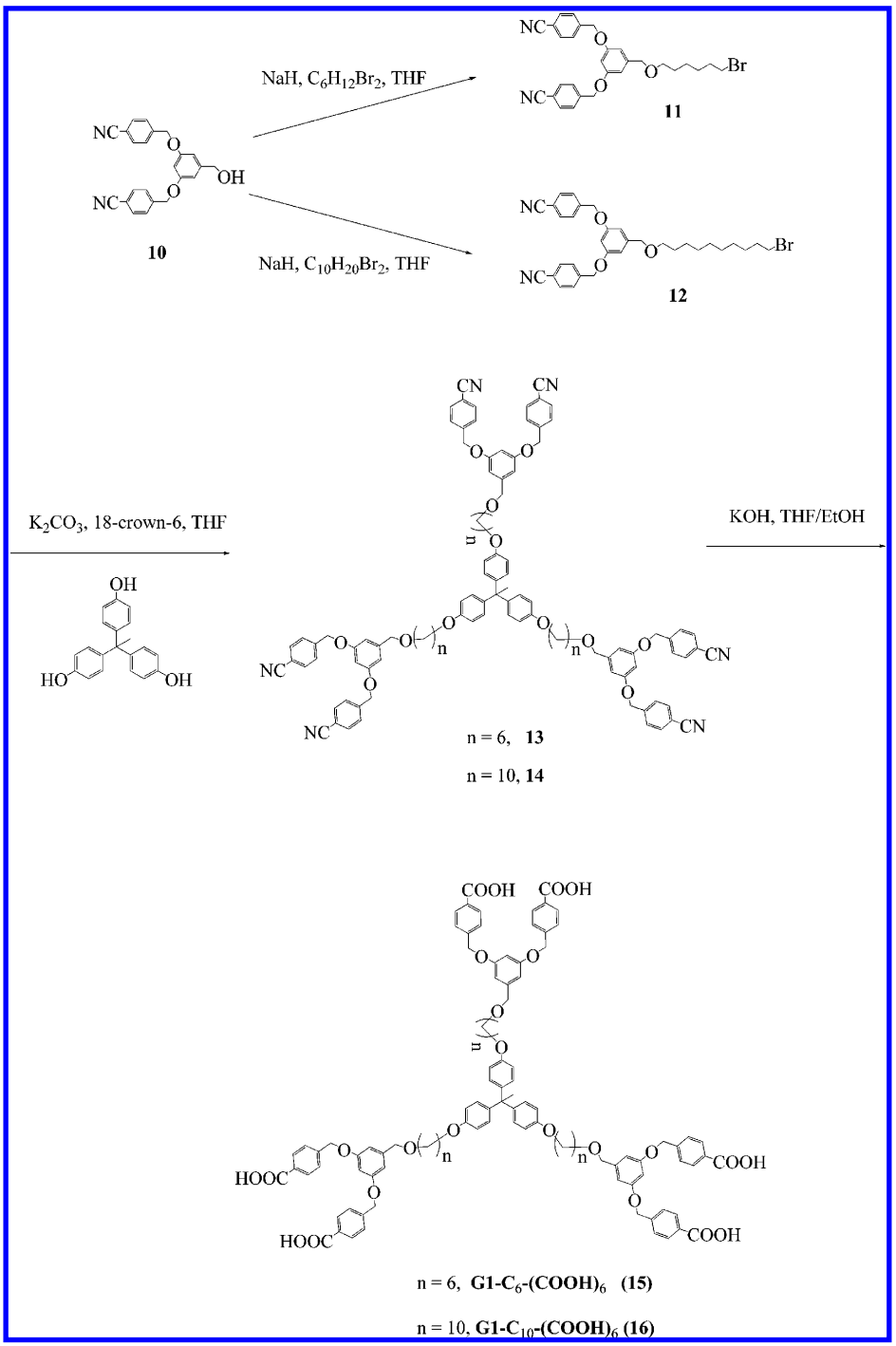

51, 63, and 72 °C, respectively. Because of higher molecular weights in the higher generations of dendrimers, the glass transition temperatures of the H-bonded dendrimers with higher generations were observed to increase monotonically. The behavior is consistent with the trends of the glass transition temperatures in earlier studied dendrimers.[31,32] As for the acceptor, **PBP-OC$_8$** (**19**) exhibits a melting temperature at 137 °C without T_g, indicating the crystalline nature of the molecule. However, H-bonds have a strong effect on the thermal properties by the introduction of OXD dendritic donors (bearing benzoic acids) to the emitting acceptor **PBP-OC$_8$** (**19**) via H-bonded self-assembly. Symmetric H-bonded dendrimers **PBP-OC$_8$/G1COOH** (**19/7**), **PBP-OC$_8$/G2COOH** (**19/8**), and **PBP-OC$_8$/G3COOH** (**19/9**) reveal distinct glass transition temperatures at 26, 48, and 65 °C, respectively, which are lower than their corresponding dendritic donors (owing to the formation of H-bonded dimers by two dendritic acids). Similar phenomena were observed in the other H-bonded dendrimers (see Table 1). The incorporation of OXD dendrons into the supramolecular structures shows no melting (only observed in POM) and crystallization peaks in DSC measurements, but T_g only. This clearly indicates that the OXD bulkly wedges in these H-bonded dendrimers effectively suppress the crystallization and reduce the chain aggregation of the emitting cores.

Another interesting trend is that all generations of dendritic analogues have the same order of transition temperatures in T_g and T_i for the H-bonded dendrimers containing the following emitting acceptors: **PBBBP-Me-OC$_8$** (**20**) > **PBP-OC$_8$** (**19**) > **PBBCN-OC$_8$** (**18**) > **PBBOC$_8$-OC$_8$** (**17**). The result of higher T_g and T_i in symmetric supramolecular dendrimers (H-bonded

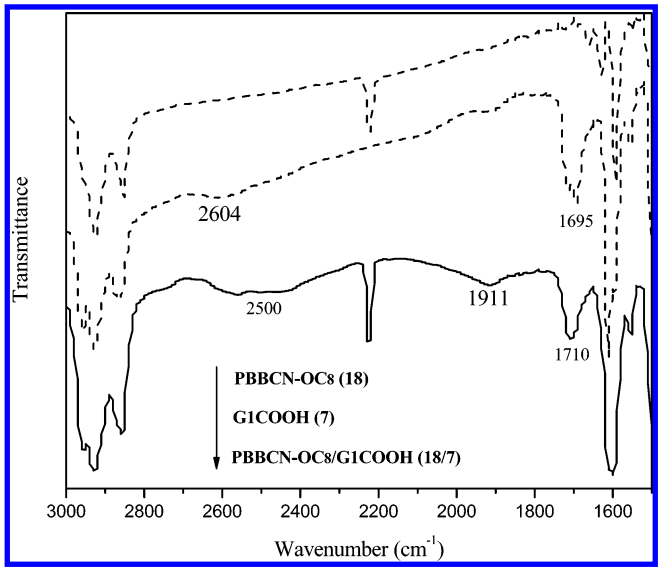

Figure 3. IR spectra of H-bonded moieties **PBBCN-OC$_8$** (**18**), **G1COOH** (**7**), and H-bonded complex **PBBCN-OC$_8$/G1COOH** (**18/7**).

Table 1. Transition Temperatures of H−Bonded Donors, Acceptors, and Dendritic Complexes

compound or H-bonded complex	T_g (°C)	T_i (°C)
G1COOH (**7**)	51	175[b]
G2COOH (**8**)	63	121[b]
G3COOH (**9**)	72	129[b]
G1-C$_6$-(COOH)$_6$ (**15**)	*a*	135[b]
G1-C$_{10}$-(COOH)$_6$ (**16**)	*a*	130[b]
PBBOC$_8$-OC$_8$ (**17**)	*a*	73
PBBOC$_8$-OC$_8$/G1COOH (**17/7**)	9	92[b]
PBBOC$_8$-OC$_8$/G2COOH (**17/8**)	37	86[b]
PBBOC$_8$-OC$_8$/G3COOH (**17/9**)	61	98[b]
PBBOC$_8$-OC$_8$/G1-C$_6$-(COOH)$_6$ (**17/15**)	*a*	85[b]
PBBOC$_8$-OC$_8$/G1-C$_{10}$-(COOH)$_6$ (**17/16**)	*a*	81[b]
PBBCN-OC$_8$ (**18**)	*a*	119
PBBCN-OC$_8$/G1COOH (**18/7**)	17	123[b]
PBBCN-OC$_8$/G2COOH (**18/8**)	43	110[b]
PBBCN-OC$_8$/G3COOH (**18/9**)	66	128[b]
PBBCN-OC$_8$/G1-C$_6$-(COOH)$_6$ (**18/15**)	*a*	92[b]
PBBCN-OC$_8$/G1-C$_{10}$-(COOH)$_6$ (**18/16**)	*a*	88[b]
PBP-OC$_8$ (**19**)	*a*	137
PBP-OC$_8$/G1COOH (**19/7**)	26	127[b]
PBP-OC$_8$/G2COOH (**19/8**)	48	120[b]
PBP-OC$_8$/G3COOH (**19/9**)	65	135[b]
PBP-OC$_8$/G1-C$_6$-(COOH)$_6$ (**19/15**)	*a*	111[b]
PBP-OC$_8$/G1-C$_{10}$-(COOH)$_6$ (**19/16**)	*a*	98[b]
PBBBP-Me-OC$_8$ (**20**)	*a*	164
PBBBP-Me-OC$_8$/G1COOH (**20/7**)	33	142[b]
PBBBP-Me-OC$_8$/G2COOH (**20/8**)	55	134[b]
PBBBP-Me-OC$_8$/G3COOH (**20/9**)	69	148[b]
PBBBP-Me-OC$_8$/G1-C$_6$-(COOH)$_6$ (**20/15**)	*a*	141[b]
PBBBP-Me-OC$_8$/G1-C$_{10}$-(COOH)$_6$ (**20/16**)	*a*	127[b]

[a] Not observed in DSC measurements. [b] The isotropization temperatures were determined by polarizing optical microscopy (POM).

trimers) containing **PBBBP-Me-OC$_8$** (**20**) and **PBP-OC$_8$** (**19**) than asymmetric supramolecular dendrimers (H-bonded dimers) containing **PBBCN-OC$_8$** (**18**) and **PBBOC$_8$-OC$_8$** (**17**) may be explained by the higher molecular weights of H-bonded trimers in the symmetric supramolecular dendrimers. Higher T_g and T_i in H-bonded dendrimer containing **PBBBP-Me-OC$_8$** (**20**) than that containing **PBP-OC$_8$** (**19**) is due to the longer central core of **PBBBP-Me-OC$_8$** (**20**). Besides, higher T_g and T_i in H-bonded dendrimer containing **PBBCN-OC$_8$** (**18**) than that containing **PBBOC$_8$-OC$_8$** (**17**) is because of the dipole−dipole interaction of CN groups in **PBBCN-OC$_8$** (**18**). In the reverse H-bonded dendrimers (containing emitting shells), e.g. **PBBBP-Me-OC$_8$** (**20**), **PBP-OC$_8$** (**19**), **PBBCN-OC$_8$** (**18**), and **PBBOC$_8$-OC$_8$** (**17**) were complexed with dendritic donor cores **G1-C$_6$-(COOH)$_6$** (**15**) and **G1-C$_{10}$-(COOH)$_6$** (**16**) in proper ratios, no phase transition peaks were found, which is probably due to the flexible chains of the polyfunctional cores in the H-bonded dendritic donors. Similar behavior in polypropylene dendrimers containing trialkoxybenzene wedges as mesogenic units was reported in the literature.[33−34]

Optical Properties. The absorption and PL spectral data of the pure chromophores (in THF and solid films) and all H-bonded dendrimers in solid films are summarized in Table 2. Figure 4a shows the absorption spectra of uncomplexed H-bond donors and acceptor **PBBCN-OC$_8$** (**18**) in THF solutions. The series of H-bonded dendrimers show very similar absorption and emission characteristics in the solid films. Figure 4b shows various asymmetric H-bonded dendrimers containing single H-bonded acceptor emitter **PBBCN-OC$_8$** (**18**) in solid films. In the asymmetric supramolecular complexes bearing dendritically mono-encapsulated chromophores, i.e., **PBBCN-OC$_8$/G1COOH** (**18/7**), **PBBCN-OC$_8$/G2COOH** (**18/8**), and **PBBCN-OC$_8$/G3COOH** (**18/9**), the absorption peak at 305 nm was attributed to the transition absorption of OXD groups and the longer absorption peak at 423 nm was attributed to the characteristic absorption of emitter **PBBCN-OC$_8$** (**18**). By increasing the generation of the dendritic donors in the H-bonded complexes, the absorbance of OXD units at 305 nm is proportional to the generation number of the dendrimers. In view of Figure 5, the PL emission spectrum of **PBBCN-OC$_8$** (**18**) showed a characteristic peak at 470 nm in THF, which is red-shifted to 512 nm in solid films due to the formation of $\pi-\pi$ stacking and molecular aggregation. In contrast to the single H-bonded acceptor emitter **PBBCN-OC$_8$** (**18**) alone, the asymmetric supramolecular dendrimers **PBBCN-OC$_8$/G1COOH** (**18/7**), **PBBCN-OC$_8$/G2COOH** (**18/8**), and **PBBCN-OC$_8$/G3COOH** (**18/9**) exhibit red-shifted PL emissions with values of λ_{max} at 554, 541, and 531 nm excited at 423 nm, respectively. This result is similar to our previous work,[25] where the photoluminescent H-bonded trimers containing bifunctional bis-pyridyl acceptors complexed with monofunctional carboxylic acids show red-shifted PL spectra as the acceptor emitters are H-bonded to donors with smaller p*Ka* values. As well-known that pH values of aqueous solutions may affect photoluminescence properties of polyelectrolytes containing pyridine units. Therefore, the H-bonded dendritic donors **G1COOH** (**7**), **G2COOH** (**8**), and **G3COOH** (**9**) bearing benzoic acid groups can be regarded as acidic solvents, so the PL spectra reveal red-shifted PL emissions compared with that of emitter **PBBCN-OC$_8$** (**18**) in THF. Interestingly, different generations of asymmetric H-bonded dendrimers containing single H-bonded acceptor emitter **PBBCN-OC$_8$** (**18**) appeared to have different degrees of red-shifted PL emissions. The red-shifts of PL emissions in asymmetric H-bonded dendrimers **PBBCN-OC$_8$/G1COOH** (**18/7**), **PBBCN-OC$_8$/G2COOH** (**18/8**), and **PBBCN-OC$_8$/G3COOH** (**18/9**) are 84, 71, and 61 nm, respectively, where the higher generations of the H-bonded dendrimers have smaller red-shifted PL emissions than the lower generations of the H-bonded dendrimers. It clearly indicates that larger dendritic wedges have higher site-isolation or dendron dilution effect than smaller dendritic ones, so the higher generations of dendrimers efficiently reduce the aggregation extent of the emitting cores. The opposite type of H-bonded dendritic complexes containing poly(alkyl aryl ether) dendrimer (dendritic donor core) complexed with a single H-bonded acceptor emitter **PBBCN-OC$_8$** (**18**) at the periphery; i.e., **PBBCN-OC$_8$/G1-C$_6$-(COOH)$_6$** (**18/**

Table 2. Photophysical Properties of H−Bonded Acceptors and Dendritic Complexes

compound or H-bonded complex	$\lambda_{PL,sol}$ (nm)	$\lambda_{PL,film}$ (nm)	$\Phi_{PL,film}$	RFI[a]
PBBOC$_8$-OC$_8$ (17)	463	468 (495)	0.09	
PBBOC$_8$-OC$_8$/G1COOH (17/7)		569	0.11	0.87
PBBOC$_8$-OC$_8$/G2COOH (17/8)		562	0.19	1.14
PBBOC$_8$-OC$_8$/G3COOH (17/9)		555	0.23	2.16
PBBOC$_8$-OC$_8$/G1-C$_6$-(COOH)$_6$ (17/15)		570	0.07	
PBBOC$_8$-OC$_8$/G1-C$_{10}$-(COOH)$_6$ (17/16)		558	0.07	
PBBCN-OC$_8$ (18)	470	512	0.08	
PBBCN-OC$_8$/G1COOH (18/7)		556	0.20	0.73
PBBCN-OC$_8$/G2COOH (18/8)		543	0.26	0.97
PBBCN-OC$_8$/G3COOH (18/9)		532	0.32	1.97
PBBCN-OC$_8$/G1-C$_6$-(COOH)$_6$ (18/15)		556	0.13	
PBBCN-OC$_8$/G1-C$_{10}$-(COOH)$_6$ (18/16)		550	0.13	
PBP-OC$_8$ (19)	460	482 (506)	0.08	
PBP-OC$_8$/G1COOH (19/7)		545	0.20	1.27
PBP-OC$_8$/G2COOH (19/8)		539	0.26	2.33
PBP-OC$_8$/G3COOH (19/9)		522	0.33	4.50
PBP-OC$_8$/G1-C$_6$-(COOH)$_6$ (19/15)		539	0.18	
PBP-OC$_8$/G1-C$_{10}$-(COOH)$_6$ (19/16)		533	0.16	
PBP-OC$_8$/G1COOCH$_3$ (19/4)		482 (506)	0.13	0.55
PBP-OC$_8$/G2COOCH$_3$ (19/5)		499	0.18	1.04
PBP-OC$_8$/G3COOCH$_3$ (19/6)		506	0.19	1.27
PBBBP-Me-OC$_8$ (20)	511	535 (567)	0.10	
PBBBP-Me-OC$_8$ /G1COOH (20/7)		607	0.16	0.39
PBBBP-Me-OC$_8$ /G2COOH (20/8)		588	0.22	1.06
PBBBP-Me-OC$_8$ /G3COOH (20/9)		568	0.32	1.61
PBBBP-Me-OC$_8$ /G1-C$_6$-(COOH)$_6$ (20/15)		610	0.09	
PBBBP-Me-OC$_8$ /G1-C$_{10}$-(COOH)$_6$ (20/16)		602	0.10	

[a] The relative fluorescent intensities (RFI) were calculated by the ratio of the core emission intensities excited at the OXD unit and the core absorption peaks.

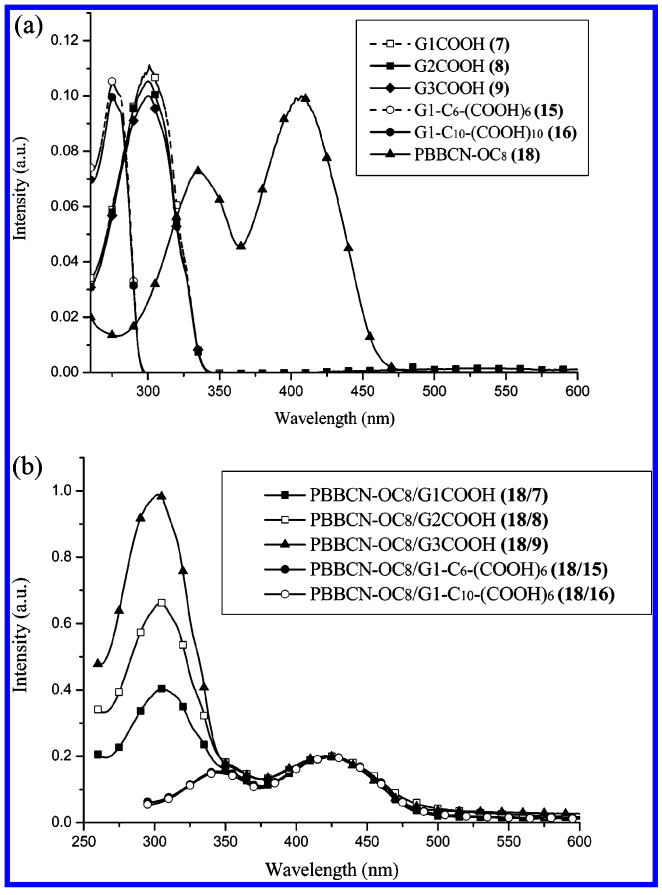

Figure 4. UV−vis absorption spectra of (a) uncomplexed H-bond donors and acceptor **PBBCN-OC$_8$** (**18**) in THF solutions and (b) **PBBCN-OC$_8$** (**18**) and its H-bonded dendrimers in solid films, which are normalized at the absorption peak of **PBBCN-OC$_8$** (**18**) at 423 nm.

15) and **PBBCN-OC$_8$/G1-C$_{10}$-(COOH)$_6$** (**18/16**), also both exhibit red-shifted emission peaks at 556 and 550 nm, respectively, compared with that of **PBBCN-OC$_8$** (**18**) in THF. With respect to **PBBCN-OC$_8$/G1-C$_6$-(COOH)$_6$** (**18/15**), the relative 6 nm blue-shift of PL emission in **PBBCN-OC$_8$/G1-C$_{10}$-(COOH)$_6$** (**18/16**) may be explained by that the longer flexible alkyl chains (as solid solvents) in the dendritic donor cores result in higher dilution effect for emitting acceptors. It is worthy noticing that the PL emission spectra of **PBBCN-OC$_8$/G1-C$_6$-(COOH)$_6$** (**18/15**) and **PBBCN-OC$_8$/G1-C$_{10}$-(COOH)$_6$** (**18/16**) are similar to that of **PBBCN-OC$_8$/G1COOH** (**18/7**), which means that poly(alkyl aryl ether) dendritic acid cores in the reverse form of the previous H-bonded dendrimers affect PL emission behavior of **PBBCN-OC$_8$** (**18**) in a similar way as the lower generation of **G1COOH** (**7**). Figure 6 shows the PL emission characteristics of emitter **PBP-OC$_8$** (**19**) and its double H-bonded dendrimers with symmetric structures. All PL emission data are summarized in Table 2, which demonstrate similar trends as those of single H-bonded acceptor emitter **PBBCN-OC$_8$** (**18**) and its asymmetric H-bonded dendrimers. Compared with single H-bonded dendrimers, no further red-shifted PL emissions were observed in the double H-bonded dendrimers due to the weaker H-bonded effect of the second H-bonds on the conjugated structures of double H-bonded acceptors and the double dilution effect from double amount of donor acids.

Because of significant overlap in the absorption spectra of the representative chromophores (compounds **17**, **18**, **19**, and **20**) and the emission spectrum of model compound **1** in Figure 7, the energy transfer from the OXD dendritic groups to the central emitters can be expected, which was also probed by photoluminescent excitation (PLE) spectra of H-bonded dendrimers containing **PBP-OC$_8$** (**19**) as shown in Figure 8. Similar spectral features of PLE spectra appear to match those of the corresponding absorption spectra, where both peaks (ca. 300 and 425 nm) exist, indicating that the peripheral OXD units in such supramolecular dendrimers possess light-harvesting capability. Hence, the functionalized OXD dendron units or the emitting core **PBP-OC$_8$** (**19**) can be independently addressed by changing the excitation wavelength. By excitation of the dendrons and the cores selectively, it provides a window to study

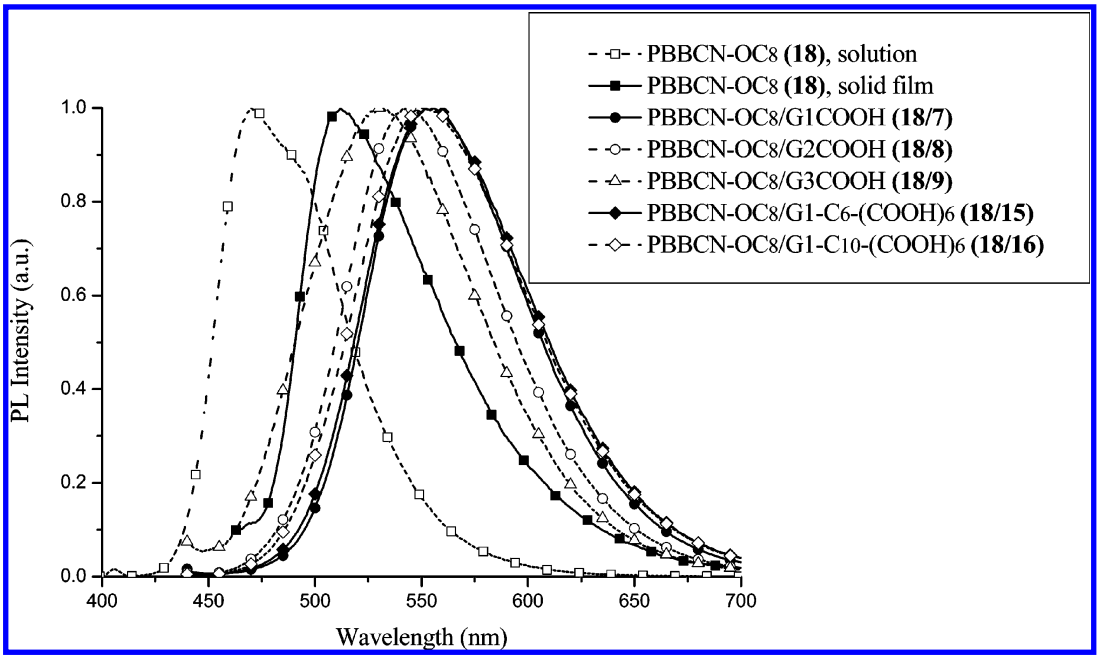

Figure 5. Normalized PL spectra of mono-pyridyl (single H-bonded) acceptor emitter **PBBCN-OC$_8$** (**18**) and its H-bonded dendrimers.

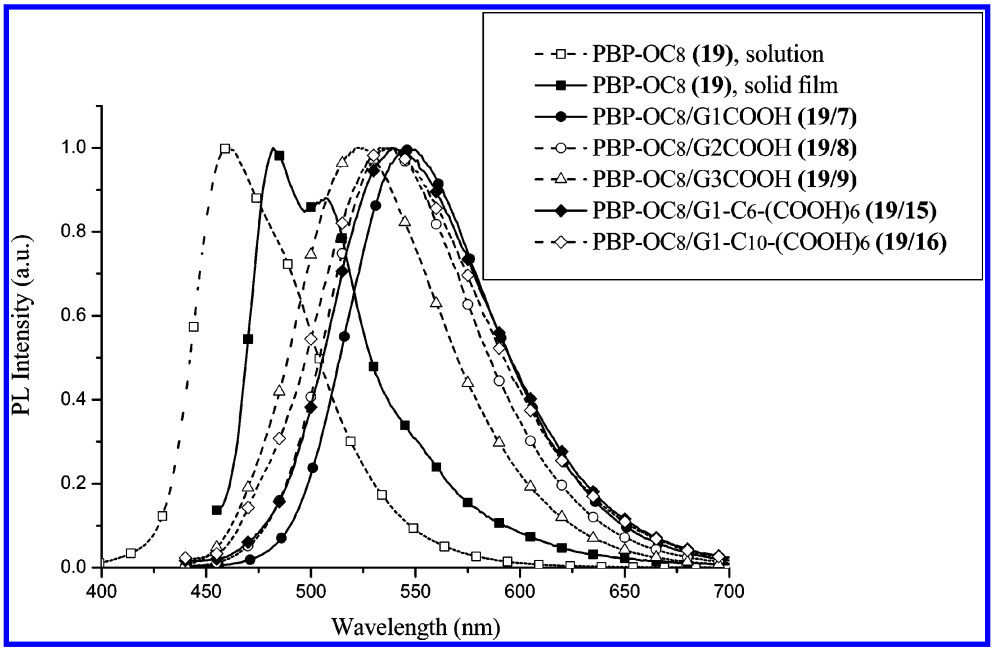

Figure 6. Normalized PL spectra of bis-pyridyl (double H-bonded) acceptor emitter **PBP-OC$_8$** (**19**) and its H-bonded dendrimers.

the photoinduced energy transfer between H-bonded donors and acceptors. As shown in Figure 9, when the dendritic OXD groups were excited at 305 nm, the symmetric H-bonded dendrimers containing **PBP-OC$_8$** (**19**), i.e., **PBP-OC$_8$/G1COOH** (**19/7**), **PBP-OC$_8$/G2COOH** (**19/8**), and **PBP-OC$_8$/G3COOH** (**19/9**), emit fluorescence at wavelengths of 545, 539, and 522 nm, respectively. The photoexcitation of H-bonded dendrimers at the maximum absorption wavelength of OXD units apparently generated identical predominant emission peaks as those excited at the maximum absorption of **PBP-OC$_8$** (**19**). Whereas, no luminescence was detected from the major emission of OXD dendron, and thus the energy transfer of OXD emission from the dendritic wedges to the central emitting cores is confirmed. In addition, the values of relative fluorescent intensities (RFI) were calculated from the intensity ratio of core emissions by respective excitations at the maximum absorption peaks of the OXD dendrons and the emitting cores (ca. 300 and 425 nm, respectively). The values of RFI from H-bonded G1 to G3 dendrimers are 1.27, 2.33, and 4.50, respectively. The results indicate that the intensity of the sensitized emission (by energy transfer from OXD dendritic absorption at 300 nm) is even stronger than that of the direct core emission (by core absorption at 425 nm) in the H-bonded dendrimers. Therefore, sensitization by the telechelic antennae is more efficient than direct excitation at the maximum absorption of the chromophore. The increasing tendency from H-bonded G1 to G3 dendrimers unambiguously suggests that the more number of grafted OXD units (higher generations) in the dendrons, the higher capability of light-harvest. However, in contrast to symmetric H-bonded (G1-G3) dendrimers containing double H-bonded acceptor emitter **PBP-OC$_8$** (**19**), where all RFI values are larger than 1 in all generations of H-bonded dendrimers, the enhancement of the core emission in the asymmetric H-bonded dendrimers containing single H-bonded acceptor emitter **PBBCN-OC$_8$** (**18**) (as

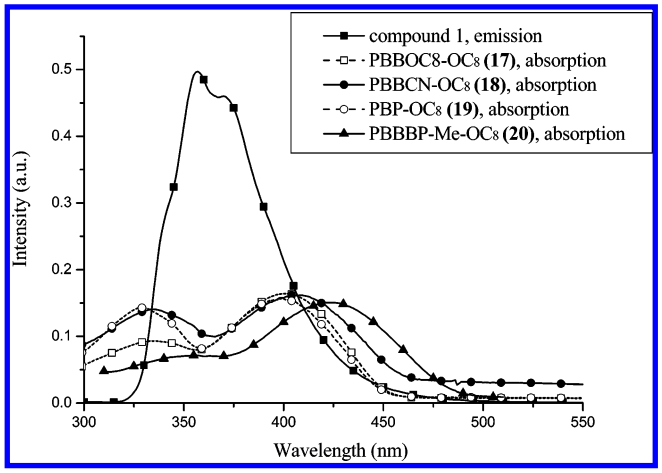

Figure 7. UV−vis absorption spectra of (single/double H-bonded) acceptor emitters **PBBOC$_8$-OC$_8$** (**17**), **PBBCN-OC$_8$** (**18**), **PBP-OC$_8$** (**19**), and **PBBBP-Me-OC$_8$** (**20**) and PL spectrum of compound **1** (containing an OXD unit) in THF. It indicates that an overlap exists between the emission band of the donor and the absorption bands of the acceptor emitters, resulting in energy transfer from OXD units to the emitting core.

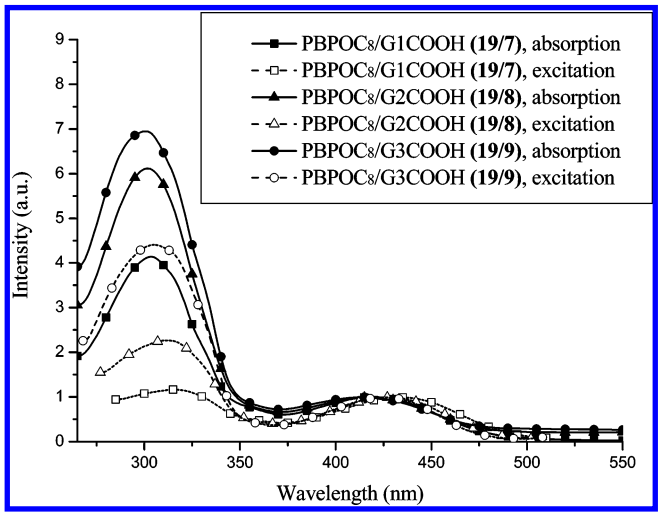

Figure 8. UV−vis absorption and corrected excitation spectra of symmetric H-bonded dendrimers (with different generations of donor dendrimers)**PBP-OC$_8$/G1COOH** (**19/7**), **PBP-OC$_8$/G2COOH** (**19/8**), and **PBP-OC$_8$/G3COOH** (**19/9**) monitored at the core of double H-bonded acceptor emitter **PBP-OC$_8$** (**19**).

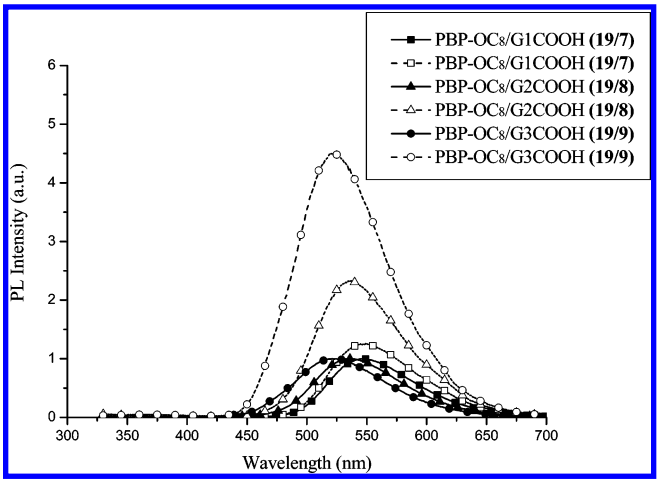

Figure 9. PL spectra of symmetric supramolecular dendrimers containing double H-bonded acceptor emitter **PBP-OC$_8$** (**19**) in thin films, which were excited at the dendritic peripheral OXD units (at 305 nm for open symbols) and at the maximum absorption of the emitting core **PBP-OC$_8$** (**19**) in H-bonded G1-G3 dendrimers (at 418, 415, 408 nm, respectively, for solid symbols).

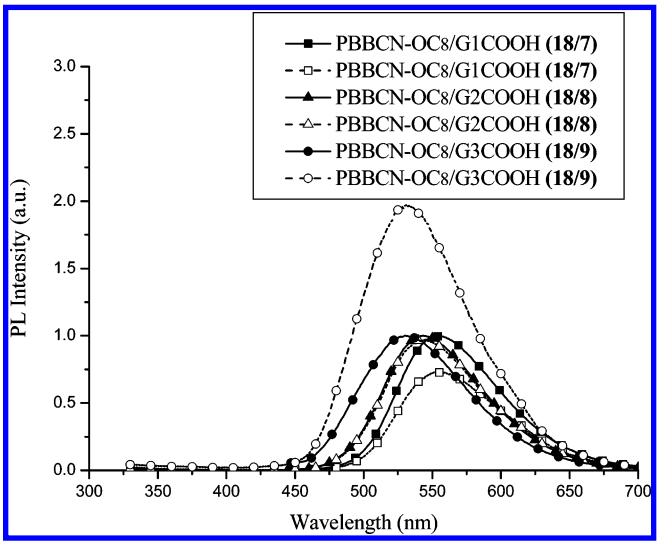

Figure 10. PL spectra of asymmetric supramolecular dendrimers containing single H-bonded acceptor emitter **PBBCN-OC$_8$** (**18**) in thin films, which were excited at the dendritic peripheral OXD units (at 305 nm for open symbols) and at the maximum absorption of the emitting core **PBBCN-OC$_8$** (**18**) in H-bonded G1-G3 dendrimers (at 424, 423, and 419 nm, respectively, for solid symbols).

excited at the maximum absorption of OXD dendron) only occurred in the third generation of H-bonded dendrimers **PBBCN-OC$_8$/G3COOH** (**18/9**) as shown in Figure 10. One of the major reasons should be attributed to that single H-bonded acceptor emitter **PBBCN-OC$_8$** (**18**) is complexed only with one H-bonded donor (energy-transfer donor) in the molar ratio of 1:1 to result in the relatively lower enhancement of fluorescent intensity, as compared with double H-bonded acceptor emitter **PBP-OC$_8$** (**19**) complexed with two H-bonded donor (energy-transfer donor) in the molar ratio of 1:2.

The possible behavior of supramolecular aggregation might be explained as shown in Figure 11. To balance the contribution of the number of OXD units in asymmetric/symmetric H-bonded dendrimers, the complexation of G1 donors with double H-bonded acceptor emitters should be comparable with the complexation of G2 donors with single H-bonded acceptor emitters as shown in Figure 11b−d, which all possess four OXD units in each asymmetric/symmetric H-bonded dendrimer. Interestingly, comparing asymmetric H-bonded dendrimers with four OXD units on one donor side of asymmetric ones and two OXD units on both donor sides of symmetric ones (or with eight OXD units on one donor side of the asymmetric ones and four OXD units on both donor sides of symmetric ones), both series of RFI values exhibit the trends in H-bonded dendrimers containing: **PBP-OC$_8$** (**19**) > **PBBOC$_8$-OC$_8$** (**17**) > **PBBCN-OC$_8$** (**18**) as the acceptor emitters **PBP-OC$_8$** (**19**), **PBBOC$_8$-OC$_8$** (**17**), and **PBBCN-OC$_8$** (**18**) were complexed with dendritic donors bearing the same number of OXD units. In terms of energy transfer, RFI values (with 4 OXD units in each H-bonded complex) are equal to 1.27, 1.14, and 0.97 in **PBP-OC$_8$/G1COOH** (**19/7**), **PBBOC$_8$-OC$_8$/G2COOH** (**17/8**), and **PBBCN-OC$_8$/G2COOH** (**18/8**), respectively, and RFI values (with eight OXD units in each H-bonded complex) are 2.33, 2.16, and 1.97 in **PBP-OC$_8$/G2COOH** (**19/8**), **PBBOC$_8$-OC$_8$/G3COOH** (**17/9**), and **PBBCN-OC$_8$/G3COOH** (**18/9**), respectively. This should be attributed to the best acceptor emitter separation by donor dendrons on both sides of the symmetric H-bonded dendrimers containing double H-bonded acceptor emitter **PBP-OC$_8$** (**19**). Moreover, comparing asymmetric H-

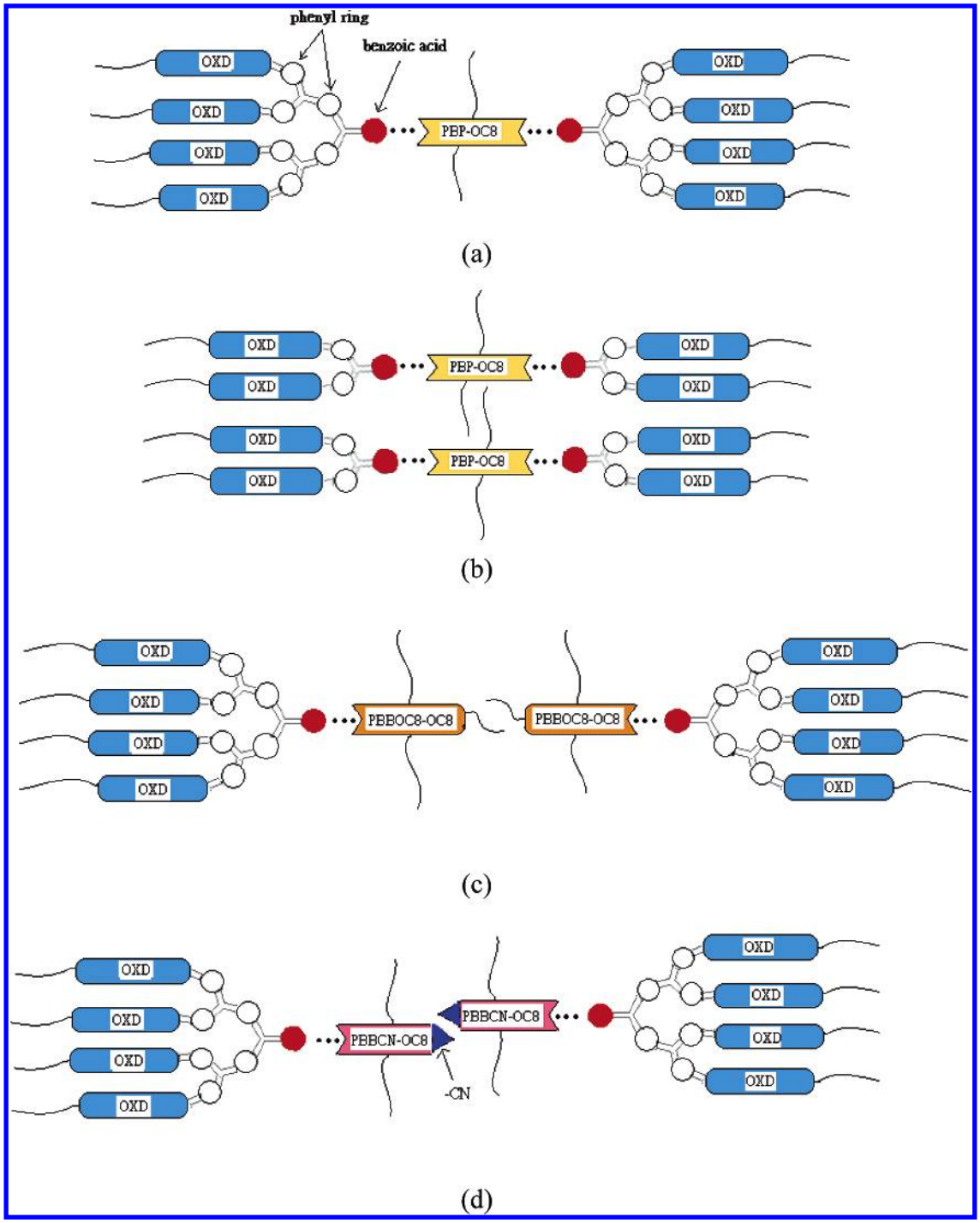

Figure 11. Schematic representation of double H-bonded encapsulation of symmetric dendrimers, (a) **PBP-OC$_8$/G2COOH** (**19/8**) and (b) **PBP-OC$_8$/G1COOH** (**19/7**), and single H-bonded encapsulation of asymmetric dendrimers, (c) **PBBOC$_8$-OC$_8$/G2COOH** (**17/8**) and (d) **PBBCN-OC$_8$/G2COOH** (**18/8**).

bonded dendrimers containing single H-bonded acceptor emitters **PBBOC$_8$-OC$_8$** (**17**) and **PBBCN-OC$_8$** (**18**), both acceptor emitters are encapsulated by single-side dendrons, but, as shown in Figure 11d, **PBBCN-OC$_8$** (**18**) in H-bonded dendrimers is further aggregated by the dipole−dipole interaction of CN groups. However, comparing symmetric H-bonded dendrimers **PBP-OC$_8$/G1COOH** (**19/7**) and **PBP-OC$_8$/G2COOH** (**19/8**) in Figure 11a,b, not only the number of the OXD units but also the distance between OXD units and the central acceptor emitter is of major concern for the energy transfer regarding the RFI value. In general, the energy transfer is highly dependent on a number of factors,[35] including the extent of aggregation, the relative orientation of the transition dipoles, the extent of the spectral overlap, and the distance between the donor and acceptor moieties. For instance, the overlap extent between the absorption spectra of the representative chromophores **PBP-OC$_8$** (**19**), **PBBOC$_8$-OC$_8$** (**17**), and **PBBCN-OC$_8$** (**18**) and the emission spectrum of model compound **1** are approximately similar in Figure 7. In corresponding study of the H-bonded dendrimers containing double H-bonded acceptor emitter **PBBBP-Me-OC$_8$** (**20**) with longer conjugation length (Figure 12), **PBBBP-Me-OC$_8$/G2COOH** (**20/8**) and **PBBBP-Me-OC$_8$/G3COOH** (**20/9**) excited at the peripheral dendritic OXD units exhibit higher fluorescent intensities than those excited at direct **PBBBP-Me-OC$_8$** (**20**) absorption, except for the lowest generation of H-bonded dendrimer **PBBBP-Me-OC$_8$/G1COOH** (**20/**

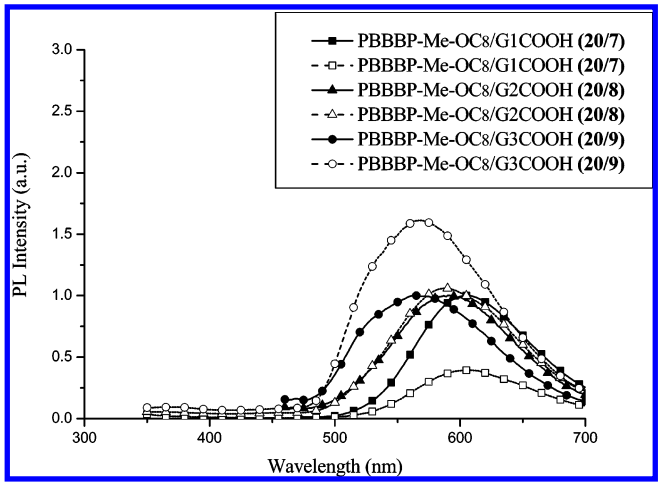

Figure 12. PL spectra of symmetric supramolecular dendrimers containing double H-bonded acceptor emitter **PBBBP-Me-OC$_8$** (**20**) in thin films as they were excited at the maximum absorption of the dendritic peripheral OXD units (at 305 nm for open symbols) and at the maximum absorption of the emitting core **PBBBP-Me-OC$_8$** (**20**) in H-bonded G1-G3 dendrimers (at 450, 446, 439 nm, respectively, for solid symbols).

7). Compared with H-bonded dendrimers containing acceptor emitter **PBP-OC$_8$** (**19**), the less spectral overlap in the emission of OXD dendrons and the absorption of **PBBBP-Me-OC$_8$** (**20**) in Figure 7 seems to explain the min reason for lower energy transfer (i.e., lower RFI values) of OXD units to chromophores in H-bonded counterparts containing acceptor emitter **PBBBP-Me-OC$_8$** (**20**).

In all H-bonded dendrimers containing emitting cores, the PL efficiencies are higher than pure chromophores and the values are much enhanced (the maximum value of 4 times larger) in the higher generation of H-bonded dendrimers, which is in accordance with the results obtained previously.[36,37] This improvement of PL efficiencies should be attributed to the bulky OXD dendrons refraining from the aggregation of chromophores. These results consistently indicate that the dendritic wedges play an important role of shielding/isolating effects among the cores. However, the PL efficiencies are not obviously improved by the complexation of chromophores with functionalized poly(alkyl aryl ether) donor dendrimers containing peripheral carboxylic acid units to form exterior emitting shells (reverse to the previous system with emitting cores). Therefore, the supramolecular anchoring of chromophores on the dendritic surface by H-bonds to form exterior emitting shells seems to be inefficient to solve the intermolecular aggregation of chromophores. Thus, the RFI values strongly depend on the types of emitters (including single/double H-bonded sites and dipole moments) and the generation number of OXD dendrons (including the number of OXD units in the H-bonded donors along with the distance between OXD units and chromophores).

To evaluate the H-bonding effect on the efficiency of energy transfer within H-bonded dendrimers, analogous dendritic mixtures without H-bonds were prepared by the esterification of the dendritic acids and then mixing with corresponding chromophores. Because of the lack of H-bonds between two components, the simple mixtures of **PBP-OC$_8$/G1COOCH$_3$** (**19/4**), **PBP-OC$_8$/G2COOCH$_3$** (**19/5**), and **PBP-OC$_8$/G3COOCH$_3$** (**19/6**) (molar ratio = 1:2, shown in Figure 13) showed similar emission spectra in contrast to **PBP-OC$_8$** (**19**) in solid films (Figure 6). These mixed systems (without H-bonds) reveal a lower ratio (the ratio of the core emissions excited at dendritic OXD units and at the core) of PL emission enhancement in comparison with those of H-bonded dendritic counterparts.

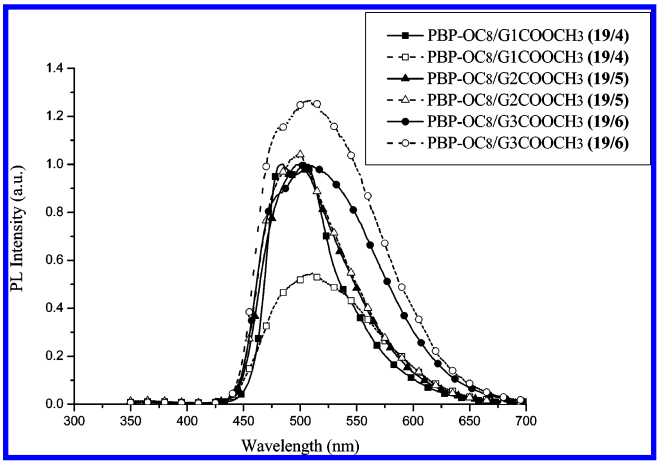

Figure 13. PL spectra of the simple mixture (without H-bonds) of **PBP-OC$_8$/G1COOCH$_3$** (**19/4**), **PBP-OC$_8$/G2COOCH$_3$** (**19/5**), and **PBP-OC$_8$/G3COOCH$_3$** (**19/6**) in thin films excited at the dendritic peripheral OXD units (at 305 nm for open symbols) and at the maximum absorption of the emitting core **PBP-OC$_8$** (**19**) in (at 425 nm for solid symbols).

Hence, **PBPOC$_8$/G1COOCH$_3$** (**19/4**), **PBP-OC$_8$/G2COOCH$_3$** (**19/5**), and **PBP-OC$_8$/G3COOCH$_3$** (**19/6**) have the relative fluorescent intensities (RFI) values of 0.55, 1.04, and 1.27, respectively. Therefore, they exhibited lower fluorescence quantum yields and RFI values than their H-bonded dendritic counterparts. The results indicate that better energy-transfer properties and higher fluorescence quantum yields are obtained as the dendritic donors are H-bonded to the emitting acceptors, where the better energy transfer is caused by higher pairing ratio and closer molecular distance between donors and acceptors through H-bonds.

Conclusions

In summary, several series of novel H-bonded dendrimers were constructed by encapsulation of chromophores with dendrimers or by complexation of functionalized poly(alkyl aryl ether) dendrimers with peripheral chromophores via supramolecular self-assembly. Various degrees of red-shifted PL emissions are expected in the H-bonded dendrimers as benzoic acids are H-bonded to the H-bonded acceptor emitters. The emission wavelengths of the mono-/bis-pyridyl (single/double H-bonded) chromophores can be easily adjusted by their surrounding H-donors. As a result, the larger (higher generation) dendritic size can afford stronger site-isolation and dendron-dilution effect, and thus the better energy-transfer and higher fluorescence quantum efficiencies can be achieved. Moreover, the peripheral OXD dendrons have specific capabilities of light-antennae and enhanced core luminescence by energy transfer from OXD dendrons. Overall, the energy transfer in the supramolecular dendrimers depends on the types of H-bonded acceptors and donors, including single/double (asymmetric/symmetric) H-bonded structures, dipole moments, dendritic generations, and the overlap ratio of the OXD emission spectra and the emitter absorption spectra. Owing to the efficient shielding effect and energy transfer of the donor dendrimers, high fluorescence quantum yields of these supramolecules have the potential to be utilized in molecular electrooptical devices.

Acknowledgment. We are thankful for the financial support from the National Science Council of Taiwan (ROC) through NSC 93-2113-M-009-011, and the instrumental support from Prof. Yu-Chie Chen (MALDI-TOF mass spectroscopy) at the Department of Applied Chemistry, National Chiao Tung University (in Taiwan).

Supporting Information Available: Text and a scheme giving procedures for the synthesis and purification of all mono-/bis-pyridyl acceptor emitters **PBBOC$_8$-OC$_8$ (17)**, **PBBCN-OC$_8$ (18)**, **PBP-OC$_8$ (19)**, **PBBBP-Me-OC$_8$ (20)**, and their intermediates. This material is available free of charge via the Internet at http://pubs.acs.org.

References and Notes

(1) Tang, C. W.; Van Slyke, S. A. *Appl. Phys. Lett.* **1987**, *51*, 913.
(2) Burroughes, J. H.; Bradley, D. D. C.; Brown, A. R.; Marks, R. N.; Mackay, K.; Friend, R. H.; Burn, P. L.; Holmes, A. B. *Nature (London)* **1990**, *347*, 539.
(3) Cao, Y.; Parker, I. D.; Yu, G.; Zhang, C.; Heeger, A. J. *Nature (London)* **1999**, *397*, 414.
(4) Liao, L. S.; Klubeck, K. P.; Tang, C. W. *Appl. Phys. Lett.* **2004**, *84*, 167.
(5) Greenham, N. C.; Moratti, S. C.; Bradley, D. D. C.; Friend, R. H.; Burn, P. L.; Holmes, A. B. *Nature (London)* **1993**, *365*, 628.
(6) Scherf, U.; List, E. J. W. *Adv. Mater.* **2002**, *14*, 477.
(7) Jin, S. H.; Kim, M. Y.; Kim, J. Y.; Lee, K.; Gal, Y. S. *J. Am. Chem. Soc.* **2004**, *126*, 2474.
(8) Jenekhe, S. A.; Osaheni, J. A. *Science* **1994**, *265*, 765.
(9) Joswick, M. D.; Cambell, I. H.; Barashkov, N. N.; Ferraris, J. P. *J. Appl. Phys.* **1996**, *80*, 2883.
(10) Weil, T.; Reuther, E.; Müllen, K. *Angew. Chem., Int. Ed.* **2002**, *41*, 1900.
(11) Herrmann, A.; Weil, T.; Sinigersky, V.; Wiesler, U.-M.; Vosch, T.; Hofkens, J.; De Schryver, F. C.; Müllen, K. *Chem.—Eur. J.* **2001**, *7*, 4844.
(12) Gronheid, R.; Hofkens, J.; Kohn, F.; Weil, T.; Reuther, E.; Müllen, K.; De Schryver, F. C. *J. Am. Chem. Soc.* **2002**, *124*, 2418.
(13) Liu, D.; De Feyter, S.; Cotlet, M.; Stefan, A.; Wiesler, U.-M.; Herrmann, A.; Grebel-Koehler, D.; Qu, J.; Müllen, K.; De Schryver, F. C. *Macromolecules* **2003**, *36*, 5918.
(14) Kwon, T. W.; Alam, M. M.; Jenekhe, S. A. *Chem. Mater.* **2004**, *16*, 4657.
(15) Wang, P. W.; Liu, Y. J.; Devadoss, C.; Bharathi, P.; Moore, J. S. *Adv. Mater.* **1996**, *8*, 237.
(16) Halim, M.; Pillow, J. N. G.; Samuel, D. W.; Burn, P. L. *Adv. Mater.* **1999**, *11*, 371.
(17) Kuwabura, Y.; Ogawa, H.; Inada, H.; Noma, N.; Shirota, Y. *Adv. Mater.* **1994**, *6*, 677.
(18) Bettenhausen, J.; Greczmiel, M.; Jandke, M.; Strohriegl, P. *Synth. Met.* **1997**, *91*, 223.
(19) Bettenhausen, J.; Strohriegl, P. *Adv. Mater.* **1996**, *8*, 507.
(20) Oldham, W. J., Jr.; Lachicotte, R. J.; Bazan, G. C. *J. Am. Chem. Soc.* **1998**, *120*, 2987.
(21) Paleos, C. M.; Tsiourvas, D. *Angew. Chem., Int. Ed. Eng.* **1995**, *34*, 1696.
(22) Kato, T.; Mizoshita, N.; Kanie, K. *Macromol. Rapid Commun.* **2001**, *22*, 797.
(23) Beginn, U. *Prog. Polym. Sci.* **2003**, *28*, 1049.
(24) Precup-Blaga, F. S.; Garcia-Martinez, J. C.; Schenning, A. P. H. J.; Meijer, E. W. *J. Am. Chem. Soc.* **2003**, *125*, 12953.
(25) (a) Lin, H. C.; Sheu, H. Y.; Chang, C. L.; Tsai, C. *J. Mater. Chem.* **2001**, *11*, 2958. (b) Lin, H. C.; Tsai, C. M.; Huang, G. H.; Tao, Y. T. *Macromolecules* **2006**, *39*, 557.
(26) Guilbault, G. G.; Ed. *Practical Fluorescence*; Marcel Dekker: New York, 1990.
(27) Wu, C. W.; Tsai, C. M.; Lin, H. C. *Macromolecules* **2006**, *39*, 4298.
(28) Fréchet, J. M. J.; Wooley, K. L.; Hawker, C. J. *J. Am. Chem. Soc.* **1993**, *115*, 11496.
(29) Hawker, C. J.; Fréchet, J. M. J. *J. Am. Chem. Soc.* **1990**, *112*, 7638.
(30) (a) Kumar, U.; Kato, T.; Fréchet, J. M. J. *J. Am. Chem. Soc.* **1992**, *114*, 663. (b) Odinokov, S. E.; Mashkovshky, A. A.; Glazunov, V. P.; Iogansen, A. V.; Rassadin, B. V. *Spectrochim. Acta* **1976**, *32A*, 1355. (c) Kato, T.; Kihara, H.; Uryu, T.; Fujishima, A.; Fréchet, J. M. J. *Macromolecules* **1992**, *25*, 6836.
(31) (a) Farrington, P. J.; Craig, J. H.; Fréchet, J. M. J.; Mackay, M. E. *Macromolecules* **1998**, *31*, 5043. (b) Stutz, H. *J. Polym. Sci., Part B: Polym. Phys.* **1995**, *33*, 333.
(32) Wooley, K. L.; Hawker, C. J.; Pochan, J. M.; Fréchet, J. M. J. *Macromolecules* **1993**, *26*, 1514.
(33) Cameron, J. H.; Facher, A.; Lattermann, G.; Diele, S. *Adv. Mater.* **1997**, *9*, 398.
(34) Precup-Blaga, F. S.; Schenning, A. P. H. J.; Meijer, E. W. *Macromolecules* **2003**, *36*, 56.
(35) Lakowicz, J. R. *Principles of fluorescence spectroscopy*; Kluwer Academic/Plenum Publishers: New York, 1999.
(36) Baines, F. L.; Billingham, N. C.; Armes, S. P. *Macromolecules* **1996**, *29*, 3416.
(37) Chen, Z. K.; Hoi Sim Lee, N.; Huang, W.; Xu, Y. S.; Cao, Y. *Macromolecules* **2003**, *36*, 1009.

MA0610358